JOURNAL OF THEORETICAL AND APPLIED MECHANICS
61, 4, pp. 783-791, Warsaw 2023
https://doi.org/10.15632/jtam-pl/171544x

THE EFFECT OF GRAPHITE FLAKE DIAMETER ON THE RESISTANCE TO THERMAL SHOCK, MICROSTRUCTURE AND MECHANICAL PROPERTIES OF SILICON CARBIDE NANOMATERIALS

Mohammed H. Mahmood
Department of Projects, University of Anbar, Iraq
e-mail: mohammed.hussein@uoanbar.iq

Wekar M. Khalaf
Mechanical Engineering Department, University of Anbar, Iraq
e-mail: wekar@uoanbar.edu.iq

Kafel Azeez
Renewable Energy Research Center, University of Anbar, Iraq
e-mail: kafelazeez1966@uoanbar.edu.iq (corresponding author)

To ascertain the impact of graphite flake diameter on the microstructure and mechanical properties as well as resistance to thermal shock, graphite flakes of various diameters have been added to zirconium dibromide (ZrB_2) 20 vol.% nano-silicon carbide (SiC) 20 vol.% graphite ($ZS_{np}G$) ceramics. The objective of this study is to investigate the effect of graphite flake diameter on silicon carbide nanomaterials. The study aims to identify a strategy for achieving high comprehensive performance of ZrB_2-based ceramics incorporating graphite for future research on ultra-high temperature ceramics (UHTCs). The dispersion of measurements has been conducted by combining a solid powder with ethanol at various mass fractions. The results demonstrated that, while no changing fracture toughness considerably, the relative density and flexural strength of $ZS_{np}G$ ceramics initially increased and then declined with graphite diameter increasing. The micro-crack length reduction due to residual thermal stress, appearance of silicon carbide nanoparticles within granulation, and management of graphite distribution all contributed significantly to the improvement of flexural strength $ZS_{np}G$ ceramics. According to the computed thermal shock parameters, $ZS_{np}G$ ceramics fracture propagation was constrained by graphite with a larger starting diameter and prevented with a finer starting diameter.

Keywords: graphite, flake diameter, thermal shock, microstructure

1. Introduction

Ultra-high temperature ceramics (UHTCs) are a family of materials made of nitrides, carbides and boron compounds of transition alloys. In applications, zirconium-based (ZrB_2) UHTCs are used in missile propulsion, recyclable atmospheric re-entry vehicles and thermoplastics. They have low density, high melting point ($> 2500^\circ$C) and resistance to chemical corrosion. One may find them employed for safety measures in hypersonic spacecraft (Xiang *et al.*, 2015; Gautam and Mohan, 2015; Wang *et al.*, 2009a; Guo, 2009).

By adding small sized silicon carbide nanoparticles (SiC_{np}), which are intragranular nano--structures, zirconium dibromide mechanical characteristics and resistance to oxidation can be greatly enhanced (Han *et al.*, 2009; Chamberlain *et al.*, 2006; Zhu *et al.*, 2007; Guo *et al.*, 2009). This method can not get over their inherent brittleness and resistance to thermal shock, which prevents them from using in harsh environments (Yang *et al.*, 2011). To address these

shortcomings, one approach that included addition of a larger phase into ceramics with ZrB_2 has been adopted (Liu *et al.*, 2010).

The use of graphite can increase reliability of brittle materials because it can stop fracture growth and release residual stress (Guo *et al.*, 2008; Liu *et al.*, 2009a). The aircraft industry has substantially increased the use of natural graphite flakes. The graphite flakes controlled ceramics ZrB_2-SiC (ZS) has been found to substantially increase thermal shock resistance while maintaining acceptable levels of oxidation resistance as reported in the available literature (Liu *et al.*, 2009b; Yang *et al.*, 2009; Hou *et al.*, 2013). Because graphite flakes in ZrB_2-SiC-graphite (ZSG) ceramics behave as defects, adding the graphite considerably reduces flexural of strength ZS ceramics.

In addition, the decrease in flexural strength take also place because graphite weakens bonding and reduces ceramics capacity to transfer load (Iao *et al.*, 2014). Therefore, it is necessary to research the impact of diameter of graphite on thermal and mechanical characteristics as well as the enhancement of flexural strength of ZrB_2-based ceramics.

The recent research has concentrated on carbon fiber reinforced ZrB_2-based ceramics because, when compared to other reinforcements, the carbon fiber offers more benefits in improving fracture toughness (Calabrese *et al.*, 2018; Zamora *et al.*, 2012) and has a high potential in significantly increasing the resistance to thermal shock.

High sintering temperature, on the other hand, causes substantial deterioration of carbon fibers in modified ZrB_2-based ceramics, impeding research on such materials. As a result, techniques to control carbon fiber degradation are essential in the production of carbon fiber reinforced ZrB_2-based ceramics. Conventional steps include decreasing the processing time, using carbon coated fibers and reducing the melting point (Zhang *et al.*, 2008). For carbon fiber reinforced ZrB_2-based ceramics, spark plasma sintering (SPS) may be advantageous because it combines the effects of rapid heating, powder cleaning of the surface, and fast consolidation of powders to theoretical density (Mishra and Pathak, 2008). Because nanosized particles have a much higher sintering occupation than micrometer powders, they are used as the base material in the conventional method of lowering the sintering temperature of ZrB_2 (Lee *et al.*, 2021).

It is important to study the effect of mechanical properties and diameter of graphite flakes on the microstructure and resistance to thermal shock of silicon carbide nanomaterials in order to achieve highly comprehensive performance of ZrB_2-based ceramics for future research on extremely-high temperature ceramics (UHTCs). This research intends to find a solution by investigating the effect of graphite diameter on ZrB_2-based ceramics. The goal of this work is to pave the way for future studies of UHTCs by outlining a plan to improve the performance of ZrB_2-based ceramics in a wide variety of applications.

2. Methods and materials

2.1. Classification

The powder as received was mixed with ethanol at various powder mass ratios to create suspensions for all measurements. PEI dosage was administered on a dry weight basis (dwb%). The pre-mixed solution with the content desired suspension was added to powder mixtures of 20% graphite and 20% nano-SiC addition to ZrB_2 with varying diameters (designated as $ZS_{np}G_1$, $ZS_{np}G_2$, and $ZS_{np}G_3$). The premixed solution has been then deflocculated ultrasonically (JYD-801, Jiatuanda Technology Co. Ltd, Shenzhen, China) at an output power. The various powder mixtures were vacuum hot pressed for 1 hour at 1750°C under a tensile stress load of 30 MPa using an implicitly heated graphite die lined with BN-coated graphene sheets after drying in a related evaporator.

2.2. Preparation

The solid particles were mixed with ethanol at different powder mass percentages to create suspensions for all measurements. Doses of PEI were reported in terms of dwb% of the powder. To achieve an appropriate dispersant concentration, a premixed solution was added to powder combinations of ZrB_2 plus 20% nano-SiC and 20% graphite with varying diameters (designated $ZS_{np}G_1$, $ZS_{np}G_2$, and $ZS_{np}G_3$), which were then ultrasonically deflocculated using a JYD-801 from Jiatuanda Technology Co.

2.3. Materials

In this study, zirconium diboride (ZrB_2), 20% nano silicon carbide (SiC), and 20% graphite flakes of different sizes were utilized. Suspensions were made by combining the powder as obtained with ethanol at varying powder mass percentages, and the PEI dose was represented as a mean dry weight percentage of the powder basis (dwb%). After being ultrasonically extracted from the human body, powder mixtures of ZrB_2 containing 20% nanoSiC and 20% graphite (named $ZS_{np}G_1$, $ZS_{np}G_2$, and $ZS_{np}G_3$) were treated with the premixed solution that had the requisite dispersant concentration.

2.4. Characterization

Microstructure, mechanical properties and thermal shock resistance of graphite-containing ZrB_2-based ceramics were studied as a function of flake diameter in this study. X-ray diffraction (XRD), scanning electron microscopy (SEM), energy dispersive spectroscopy (EDS) and transmission electron microscopy (TEM) were all used to evaluate the materials. We tested flexural strength and Vickers hardness of the samples to get a sense of their mechanical qualities. The ability of samples to withstand a sudden temperature drop was measured by quenching them with cold water.

3. Discussion of results

3.1. Tests characteristics

SEM images of $ZS_{np}G$ ceramic reveal where the materials have been fractured. In this study, the microstructure features and mechanical properties of the ceramics were examined using these micrographs.

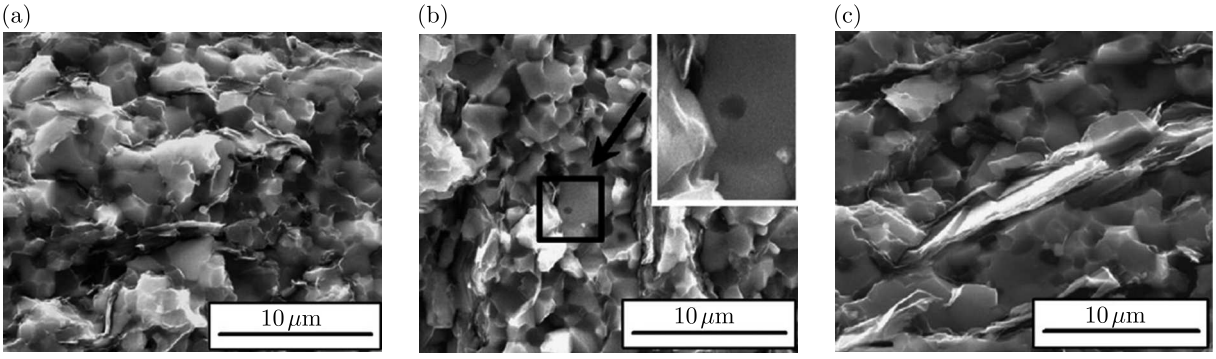

Fig. 1. Micrograph SEM of $ZS_{np}G$ ceramic fracture surfaces

Standard scanning electron micrographs (SEM) of $ZS_{np}G$ ceramic fracture surfaces are shown in Fig. 1. Nano-SiC particles may be seen within individual ZrB_2 grains in high-magnification

SEM images (Fig. 1b, arrow). Natural graphite flakes in $ZS_{np}G$ ceramics possessed basic planes perpendicular to the hot pressing direction, and the flakes diameters on fracture surfaces were similar to those found in raw graphite. When the graphite diameter was increased to 20 μm, the relative density of $ZS_{np}G$ ceramics dropped down to 98.7%. Due to the increased sintering driving force (Lv *et al.*, 2006), fine ZrB_2, ZrC, and SiC particles were produced in situ on the particle surface. A decrease in surface free energy increases density. Due to smaller contact area between graphite flakes and ceramic particles, sintering and driving forces were diminished when the graphite diameter was increased to 20 μm. The relative density of $ZS_{np}G$ ceramics was reduced as a result.

The conclusion is that the microstructure and mechanical characteristics of graphite-containing ZrB_2-based ceramics were significantly influenced by the diameter of graphite flakes. The study discovered that increasing the diameter of graphite flakes caused weaker bonding inside the $ZS_{np}G$ composite, which resulted in pits and microcracks reducing the flexural strength (Zhang *et al.*, 2009). Furthermore, a decrease in the relative density was observed when the diameter of graphite was increased to 20 μm. It was because there was less contact space between the graphite flakes and ceramic particles. $ZS_{np}G$ ceramics showed good thermal shock resistance, according to this investigation.

Adding graphite to the ceramics weakened it because weak interfaces occurred, which lowered flexural strength (Wang *et al.*, 2011). Thus, as in $ZS_{np}G_1$, the flexural strength was considerably reduced and the graphite dispersion capacity increased with lowered graphite diameter.

Table 1. $ZS_{np}G$ ceramics containing graphite flakes with different diameters and the resulting differences in mechanical characteristics and relative densities (Wang *et al.*, 2009b)

Materials	Fracture toughness [MPa·$\sqrt{\text{m}}$]	Young's modulus [GPa]	Flexural strength [MPa]	Relative density [%]
$ZS_{np}G_1$	4.31 ± 0.11	330.89 ± 19.43	451.93 ± 23.21	99.4
$ZS_{np}G_2$	4.54 ± 0.15	356.82 ± 24.64	523.06 ± 18.52	100
$ZS_{np}G_3$	4.06 ± 0.19	306.52 ± 27.96	405.58 ± 19.63	98.7

During the polishing process of $ZS_{np}G$ ceramics, a significant amount of graphite was pulled out from the composite, resulting in weaker bonding within the $ZS_{np}G$ composite. This was revealed by SEM micrographs of polished surfaces shown in Figs. 2 and 3. The diameter of pits caused by the removal of graphite grew along with the size of graphite crystals. During the flexural strength test, those holes acted as gaps causing stress concentration and a subsequent decrease in strength. Therefore, a considerable reduction in flexural strength in $ZS_{np}G_3$ might be because of a combination of microcracks and pits created by a considerable graphite pullout during polishing.

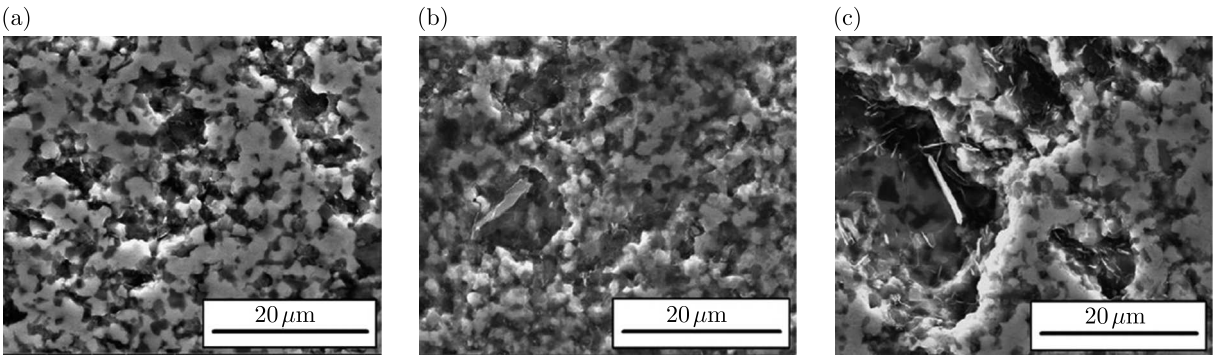

Fig. 2. Polished surfaces SEM micrographs for parallel specimens

The flexural strength of $ZS_{np}G$ ceramics cannot be solely based on the size of graphite. The flexural strength of $ZS_{np}G$ ceramics increased for diameters from 5 μm to 10 μm and then decreased from 10 μm to 20 μm, while fracture toughness did not change significantly. This was because adding the graphite to ceramics weakened it due to weak interfaces that occur, which lowered the flexural strength. However, increasing the diameter of graphite flakes could improve the mechanical properties up to a certain point by enhancing crack deflection and bridging mechanisms. Beyond this point, further increamente in graphite flake size led to weaker bonding within the composite and smaller flexural strength. Therefore, other factors such as microstructure characteristics and processing conditions also play a significant role in determining the mechanical properties of $ZS_{np}G$ ceramics (Zhang *et al.*, 2009).

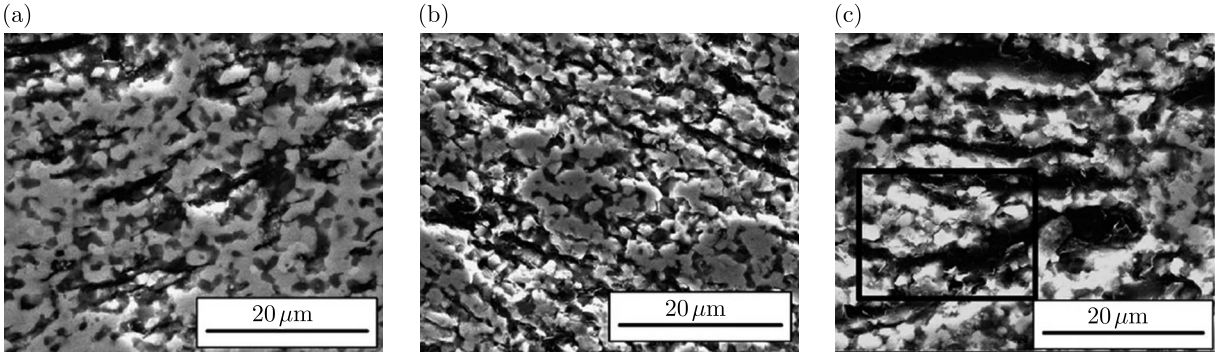

Fig. 3. SEM micrographs of polished surfaces

The perpendicular polished surfaces of $ZS_{np}G$ specimens with graphite of various sizes are depicted in micrographs in Fig. 3. In Figs. 3a and 3b, there were no discernible microcracks, but in Fig. 3c, a lengthy microcrack was discovered at the intersection of SiC and/or ZrB_2 and graphite. These properties demonstrated that the thermal residual stress and density of preexisting connecting cracks were also reduced as the graphite diameter decreased, which was consistent with subsequent studies on magnesium sulphate composites (Wang *et al.*, 2011). The source of longer cracks are the larger particles, while finer particles caused shorter break propagation distances from the particle. According to that theory, large-diameter graphite in $ZS_{np}G_3$ would result in microcracks formation, which was the primary cause of the decline in flexural strength and relative density (Liu *et al.*, 2010).

3.2. Thermal shock behavior

Figure 4 depicts the strength and stiffness of $ZS_{np}G$ ceramics after and before thermal shock at various temperatures. The modulus of elasticity of $ZS_{np}G_1$ and $ZS_{np}G_2$ ceramics was found to be greatly increased for a growth of the thermomechanical temperature difference up to 398°C. Thermal shock behavior of $ZS_{np}G$ ceramics was investigated by estimating the flexural strength drop caused by rapid quenching of test specimens from extremely high temperatures. The samples were heated in an electric resistance furnace for 15 minutes at a specific temperature before being placed in a 20°C water bath. After the thermal shock, all specimens were examined for preserved flexural strength. The study discovered that $ZS_{np}G$ ceramics have a good thermal shock resistance, which is important for materials used in high-temperature applications with fast temperature variations.

Statistically, the force of thermal shock is similar to the initial force. However, $ZS_{np}G_1$ and $ZS_{np}G_2$ ceramics showed a significant decrease in flexural strength when quenched from 400°C to 450°C. However, the dropping trend of flexural strength of $ZS_{np}G_3$ during water quenching varied from that of $ZS_{np}G_1$ and $ZS_{np}G_2$.

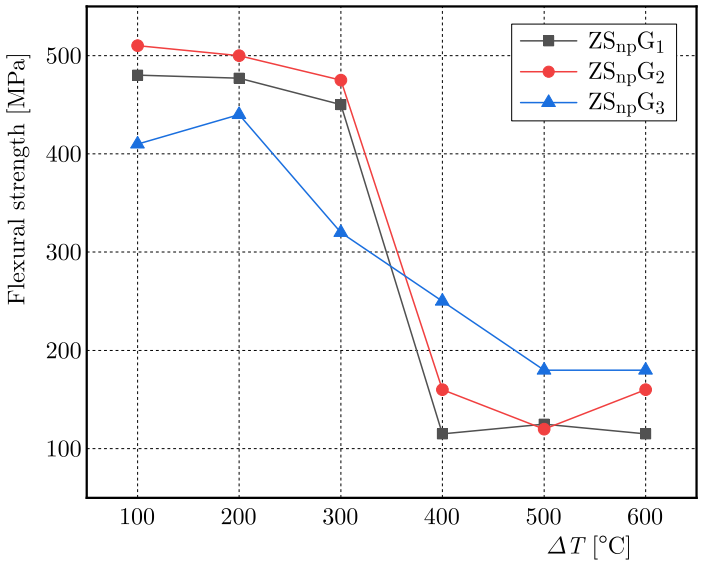

Fig. 4. The effect of temperature difference on retained strength

The researchers investigated the thermal shock response of $ZS_{np}G$ ceramics with graphite flakes of different diameters and concluded that the critical temperature differences did not suggest that they had the same thermal shock reaction. Therefore, it is important to consider other factors such as microstructure characteristics and processing conditions when evaluating the $ZS_{np}G$ ceramics thermal shock behavior.

Above $T = 350°C$, the $ZS_{np}G_3$ curve displayed a typical decrease in flexural strength owing to unstable fracture propagation that might occur occasionally in $ZS_{np}G_3$ ceramics. The considerable loss of flexural strength and lower starting temperature of that loss after water quenching revealed that the unstable fracture propagation may might occasionaly occur in $ZS_{np}G_3$ ceramics. This was because a higher thermal residual stress could be induced by a bigger diameter of graphite, which had been investigated before. The energy dissipation and deflection or pinning of a fracture occurred as it propagated through a field of residual thermal stress. Therefore, the response to thermal shock of $ZS_{np}G$ ceramics with graphite flakes of varying sizes was influenced by multiple factors such as microstructure characteristics, processing conditions and thermal residual stress induced by the graphite flakes (Mishra and Pathak, 2008).

As defined in ASTM C1525-04 (Lv *et al.*, 2006), the critical difference in temperature is determined by employing a linear regression among sites which initially reduced the average flexural strength of dampened rods to 32% as the mean material strength. All three critical temperatures found for $ZS_{np}G_1$, $ZS_{np}G_2$, and $ZS_{np}G_3$ were higher than 379°C recorded for the SiC ceramics containing 15% ZrB_2 (Lee *et al.*, 2021). Furthermore, the fact that both materials have the same critical temperature difference does not imply that they have the same response to thermal shock.

The trend of decreasing flexural strength of $ZS_{np}G_3$ after water quenching differed from that of $ZS_{np}G_1$ and $ZS_{np}G_2$ as the critical temperature differences did not imply that they had the same sensitivity to thermal shock. The study looked for a thermal shock response of $ZS_{np}G$ ceramics with varied sizes of graphite flakes and discovered that while $ZS_{np}G_1$, $ZS_{np}G_2$, and $ZS_{np}G_3$ had similar critical temperature differences, their decreasing patterns in flexural strength were different following water quenching. This was due to the fact that the microstructure features and processing circumstances of each ceramic differed, influencing their thermal shock response. As a result, numerous aspects must be considered when analyzing the thermal shock response of $ZS_{np}G$ ceramics with varied diameters of graphite flakes (Zhang *et al.*, 2008). The

fracture resistance thermal stress was calculated by multiplying the material strength σ, Young's modulus E, Poisson's ratio ν and coefficient of thermal expansion α.

The maximum temperature difference that can occur before cracks start to form is predicted by a thermal shock parameter R. It is evident that materials with significant strength and heat conductivity, as well as low values of thermal expansion and Young's modulus, can achieve a high resistance to fracture induction (Mishra and Pathak, 2008)

$$R = \frac{1-\nu}{E\alpha} \qquad R^{IV} = \frac{K_{IC}^2}{\sigma^2(1-\nu)} \tag{3.1}$$

where σ is the material strength, ν is Poisson's ratio and K_{IC} is toughness of fracture, respectively. R^{IV} determines resistance of the ceramics to catastrophic fracture propagation with the critical crucial temperature difference. In terms of the parameter R^{IV}, higher resistance to thermal shock is dependent on the ratio of Poisson's to toughness as well as lower strength of the material (Gautam and Mohan, 2015).

As can be seen in Fig. 4, the trend of impact of temperature difference on the retained strength curves for $ZS_{np}G_1$ and $ZS_{np}G_2$ is the same. The study searched for the thermal shock response of $ZS_{np}G$ ceramics with varied diameters of graphite flaked and discovered that the trend of retained strength vs. temperature difference curves for $ZS_{np}G_1$ and $ZS_{np}G_2$ is the same. Therefore, only the thermal shock parameter of $ZS_{np}G_2$ was used to compare with that of $ZS_{np}G_3$. However, it is important to note that although their trends were similar, the fracture initiation parameters were different, which affected the starting temperature of loss of flexural strength during thermal shock.

The coefficient of thermal expansion and Poisson's ratio of $ZS_{np}G$ were assumed to be of the same in order to ease computation since they are thought to have similar compositions. Therefore, the elevated R value can mostly be attributed to the exceptional flexural strength of $ZS_{np}G_2$. The computed crack propagation parameter R^{IV} of $ZS_{np}G_2$ was about 33% bigger than that of $ZS_{np}G_2$, showing that the propagation of cracks was impeded in $ZS_{np}G_3$ ceramics.

The moderate loss of flexural strength and lower ending temperature of strength reduction after water quenching suggested that unstable fracture propagation might occur occasionally in $ZS_{np}G_3$ ceramics (Fig. 4). A higher residual thermal stress could be induced by a bigger diameter of graphite, which had been investigated previously. The energy dissipation and deflection or pinning of a fracture occurred as it propagated through the field of residual thermal stress. As a graphite particle was driven during fracture propagation, interfacial friction between the graphite and other components was caused by the residual thermal stress. Meanwhile, at the edges of SiC particles, fracture deflection occurred, and considerable residual stresses during sliding and cracking used more energy of crack propagation (Liu *et al.*, 2010). This was due to the fact that the boundary of graphite flakes was a weak interlayer.

A little distinction may also be seen between $ZS_{np}G_1$ and $ZS_{np}G_2$ in terms of their thermal shock resistance parameters. In spite of this, $ZS_{np}G_1$ remained in the same mode of the thermal shock resistance as $ZS_{np}G_2$. The critical graphite size may be postulated if diameter of the graphite remains constant. It stays less than the essential diameter because the thermal shock behavior of $ZS_{np}G$ ceramics changes significantly if the graphite has a diameter larger than the critical one. This study examined the thermal shock response of $ZS_{np}G$ ceramics using graphite flakes of various sizes, and it was discovered that larger diameter flakes can stop cracks from spreading in $ZS_{np}G$ ceramics while smaller flakes can stop cracks from originating at all. In order to fully comprehend the fundamental process underlying those phenomena, additional investigation and theoretical study are required. Therefore, based on the experimental findings, a critical graphite size may be proposed, but additional research is required to completely understand its role.

4. Conclusions

The study undertaken investigates the response to thermal shock of $ZS_{np}G$ ceramics with graphite flakes of varying sizes, and the conclusions can be summarized as:

- The lower the residual thermal stress and pre-existing connecting contribution of fractures, the smaller graphite diameter.
- Longer cracks were induced by larger particles, while finer particles caused shorter break propagation lengths. As a result, a large-diameter graphite in $ZS_{np}G_3$ would produce microcracks, which was the principal source of decrease in bending strength and relative density. The presence of intragranular nano-sized SiC particles, regulation of graphite dispersion and shortening of microcrack length were all responsible for the increase in flexural strength.
- Bigger diameter graphite could slow the spread of cracks in $ZS_{np}G$ ceramics, whereas smaller diameter graphite were more effective at preventing crack initiation.
- Although $ZS_{np}G_1$, $ZS_{np}G_2$, and $ZS_{np}G_3$ had similar critical temperature differences, their decreasing trends in flexural strength were different during water quenching due to different microstructure characteristics and processing conditions.
- It is important to consider multiple factors when evaluating the thermal shock response of $ZS_{np}G$ ceramics with graphite flakes of varying sizes.

Overall, these findings suggest that controlling the graphite size and distribution can significantly impact the thermal shock behavior and mechanical properties of $ZS_{np}G$ ceramics.

References

1. Calabrese L., Brancato V., Palomba V.V., Frazzica A., Cabeza L.F., 2019, Magnesium sulphate-silicone foam composites for thermochemical energy storage: Assessment of dehydration behaviour and mechanical stability, *Solar Energy Materials and Solar Cells*, **200**, 109992
2. Chamberlain A.L., Fahrenholtz W.G., Hilmas G.E., 2006, Low-temperature densification of zirconium diboride ceramics by reactive hot pressing, *Journal of the American Ceramic Society*, **89**, 12, 3638-3645
3. Gautam G., Mohan A., 2015, Effect of ZrB_2 particles on the microstructure and mechanical properties of hybrid (ZrB_2+Al3Zr)/AA5052 insitu composites, *Journal of Alloys and Compounds*, **649**, 174-183
4. Guo S.Q., 2009, Densification of ZrB_2-based composites and their mechanical and physical properties: a review, *Journal of the European Ceramic Society*, **29**, 6, 995-1011
5. Guo S.Q., Yang J.M., Tanaka H., Kagawa Y., 2008, Effect of thermal exposure on strength of ZrB_2-based composites with nano-sized SiC particles, *Composites Science and Technology*, **68**, 14, 3033-3040
6. Guo W.M., Yang Z.G., Vleugels J., Zhang G.J., 2012, Effect of pressure loading cycle on spark plasma sintered ZrB_2-SiC-Yb_2O_3 ceramics, *Ceramics International*, **38**, 6, 5293-5297
7. Han W., Li G., Zhang X., Han J., 2009, Effect of AlN as sintering aid on hot-pressed ZrB_2-SiC ceramic composite, *Journal of Alloys and Compounds*, **471**, 1-2, 488-491
8. Hou Y., Hu P., Zhang X., Gui K., 2013, Effects of graphite flake diameter on mechanical properties and thermal shock behavior of ZrB_2-nanoSiC-graphite ceramics, *International Journal of Refractory Metals and Hard Materials*, **41**, 133-137
9. Lee J.Y., Nagalingam A.P., Yeo S.H., 2021, A review on the state-of-the-art of surface finishing processes and related ISO/ASTM standards for metal additive manufactured components, *Virtual and Physical Prototyping*, **16**, 1, 68-96

10. Liu Q., Han W., Han, J., 2010, Influence of SiCnp content on the microstructure and mechanical properties of ZrB_2-SiC nanocomposite, *Scripta Materialia*, **63**, 6, 581-584

11. Liu Q., Han W., Hu P., 2009a, Microstructure and mechanical properties of ZrB_2-SiC nanocomposite ceramic, *Scripta Materialia*, **61**, 7, 690-692

12. Liu Q., Han W., Zhang X., Wang S., Han J., 2009b, Microstructure and mechanical properties of ZrB_2-SiC composites, *Materials Letters*, **63**, 15, 1323-1325

13. Lv Y., Wen G., Lei T.Q., 2006, Tribological behavior of W2B5 particulate reinforced carbon matrix composites, *Materials Letters*, **60**, 4, 541-545

14. Mishra S.K., Pathak L.C., 2008, Effect of carbon and titanium carbide on sintering behaviour of zirconium diboride, *Journal of Alloys and Compounds*, **465**, 1-2, 547-555

15. Wang Y., Liang J., Han W., Zhang X., 2009, Mechanical properties and thermal shock behavior of hot-pressed ZrB_2-SiC-AlN composites, *Journal of Alloys and Compounds*, **475**, 1-2, 762-765

16. Wang Z., Wang S., Zhang X., Hu P., Han W., Hong C., 2009, Effect of graphite flake on microstructure as well as mechanical properties and thermal shock resistance of ZrB_2-SiC matrix ultrahigh temperature ceramics, *Journal of Alloys and Compounds*, **484**, 1-2,390-394

17. Wang Z., Wu Z., Shi G., 2011, Fabrication, mechanical properties and thermal shock resistance of a ZrB_2-graphite ceramic, *International Journal of Refractory Metals and Hard Materials*, **29**, 3, 351-355

18. Xiang L., Cheng L., Shi L., Yin X., Zhang L., 2015, Mechanical and ablation properties of laminated ZrB_2-SiC/BN ceramics, *Journal of Alloys and Compounds*, **638**, 261-266

19. Xiao K., Guo Q., Liu Z., Zhao S., Zhao, Y., 2014, Influence of fiber coating thickness on microstructure and mechanical properties of carbon fiber-reinforced zirconium diboride based composites, *Ceramics International*, **40**, 1, 1539-1544

20. Yang F., Zhang X., Han J., Du S., 2008, Mechanical properties of short carbon fiber reinforced ZrB_2-SiC ceramic matrix composites, *Materials Letters*, **62**, 17-18, 2925-2927

21. Yang H., Zhang L., Guo X., Zhu X., Fu X., 2011, Pressureless sintering of silicon carbide ceramics containing zirconium diboride, *Ceramics International*, **37**, 6, 2031-2035

22. Zamora V., Ortiz A.L., Guiberteau F., Nygren M., 2012, Crystal-size dependence of the spark-plasma-sintering kinetics of ZrB_2 ultra-high-temperature ceramics, *Journal of the European Ceramic Society*, **32**, 2, 271-276

23. Zhang X., Xu L., Du S., Liu C., Han J., Han W., 2008, Spark plasma sintering and hot pressing of ZrB_2-SiCW ultra-high temperature ceramics, *Journal of Alloys and Compounds*, **466**, 1-2, 241-245

24. Zhang X.H., Wang Z., Hu P., Han W.B., Hong C.Q., 2009, Mechanical properties and thermal shock resistance of ZrB_2-SiC ceramic toughened with graphite flake and SiC whiskers, *Scripta Materialia*, **61**, 8, 809-812

25. Zhu S., Fahrenholtz W.G., Hilmas G.E., 2007, Influence of silicon carbide particle size on the microstructure and mechanical properties of zirconium diboride-silicon carbide ceramics, *Journal of the European Ceramic Society*, **27**, 4, 2077-2083

Manuscript received May 4, 2023; accepted for print July 31, 2023